THE JOURNAL OF PHYSICAL CHEMISTRY B
A JOURNAL OF THE AMERICAN CHEMICAL SOCIETY

pubs.acs.org/JPCB

Article

Perchlorinated Triarylmethyl Radical 99% Enriched ^{13}C at the Central Carbon as EPR Spin Probe Highly Sensitive to Molecular Tumbling

Justin L. Huffman, Martin Poncelet, Whylder Moore, Sandra S. Eaton, Gareth R. Eaton, and Benoit Driesschaert*

Cite This: *J. Phys. Chem. B* 2021, 125, 7380–7387

Read Online

ACCESS | Metrics & More | Article Recommendations | Supporting Information

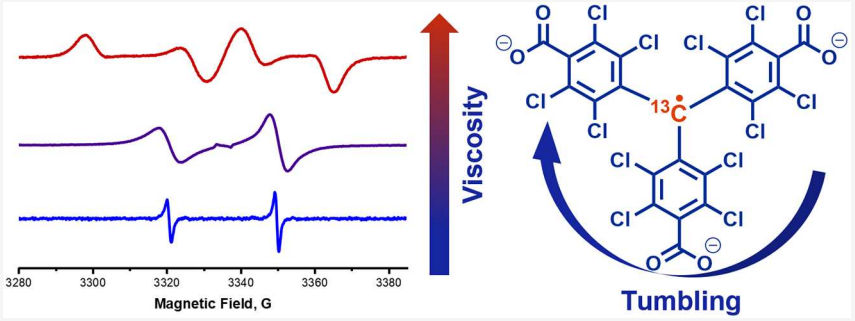

ABSTRACT: Soluble stable radicals are used as spin probes and spin labels for in vitro and in vivo electron paramagnetic resonance (EPR) spectroscopy and imaging applications. We report the synthesis and characterization of a perchlorinated triarylmethyl radical enriched 99% at the central carbon, **$^{13}C_1$–PTMTC**. The anisotropy of the hyperfine splitting with the $^{13}C_1$ (A_x = 26, A_y = 25, A_z = 199.5 MHz) and the g (g_x = 2.0015, g_y = 2.0015, g_z = 2.0040) are responsible for a strong effect of the radical tumbling rate on the EPR spectrum. The rotational correlation time can be determined by spectral simulation or via the line width or the apparent A_z after calibration, so the spin probe **$^{13}C_1$–PTMTC** can be used to measure media microviscosity with high sensitivity.

INTRODUCTION

Stable radicals such as nitroxides or triarylmethyls (TAMs or trityls) have been utilized extensively as spin probes and spin labels for in vitro and in vivo biomedical electron paramagnetic resonance (EPR) spectroscopy and imaging. Specially designed nitroxides and trityls with spectral sensitivity to various parameters such as oxygen concentration,[1] pH,[2,3] thiol concentration,[3] viscosity,[4] polarity,[5] redox status,[6] or reactive oxygen species (ROS)[7,8] have been developed. In a living system, microviscosity is an essential parameter that can modulate the rate of reactions controlled by diffusion. Abnormal microviscosity levels have been reported in many pathologies.[9] We recently devised a tetrathiatriarylmethyl radical labeled 99% at the central carbon ($^{13}C_1$), namely, $^{13}C_1$-deuterated Finland trityl or **$^{13}C_1$-dFT** (Figure 1), whose EPR spectrum is highly sensitive to molecular tumbling and, therefore, to the media microviscosity.[10,11] This sensitivity arose from the strong anisotropy of the hyperfine coupling to the $^{13}C_1$ (A_x = A_y = 17, A_z = 162 MHz) that is not entirely averaged out by molecular tumbling, even in a low-viscosity medium such as water at room temperature. Below a microviscosity of 6 cP, the spectrum of **$^{13}C_1$-dFT** is a doublet, and the effect of viscosity is a line broadening (820 mG/cP at X-band, 9.5 GHz) affecting both lines equally because of the minimal g anisotropy of the probe (g_x = 2.0033, g_y = 2.0032, g_z = 2.00275). We demonstrated that this water-soluble radical could be used in vitro, ex vivo, and in vivo to measure microviscosity by EPR.[12] Perchlorinated triarylmethyl radicals constitute another class of trityls used in

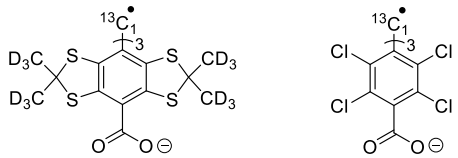

Figure 1. Structure of two $^{13}C_1$-enriched trityl radicals sensitive to molecular tumbling.

Received: April 27, 2021
Revised: June 3, 2021
Published: July 2, 2021

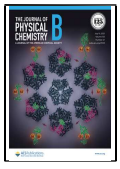

biomedical EPR to measure oxygen in vivo,[13,14] detect superoxide[15,16] or hydroxyl radical,[17] and as hyperpolarizing agents for a dynamic nuclear polarization (DNP)[18,19] or in material sciences.[20,21] A perchlorotriarylmethyl tricarboxylic acid radical (**PTMTC**) 50% enriched $^{13}C_1$ was reported recently by Elewa et al.[22] The authors showed that the line widths of the doublet arising from the hyperfine interaction with the $^{13}C_1$ were also strongly sensitive to viscosity. Moreover, the viscosity-induced line broadening did not affect the two lines equally at X-band, with a more substantial effect on the low-field peak. However, the characterization of the anisotropy of the hyperfine splitting and g tensor responsible for this spectral sensitivity to the tumbling rate of the radical was not provided, nor the characterization of the tumbling correlation times (τ_R) of the radical with the media microviscosity. We now report the synthesis of a 99% enriched **$^{13}C_1$−PTMTC**, and its EPR characterization as a probe to measure microviscosity and molecular interaction.

METHODS

General. NMR spectra were recorded using a Jeol ECZ 400S NMR spectrometer (400 MHz), then processed with MestReNova 14. EPR spectra in water and glycerol/water mixtures were recorded at West Virginia University using a Bruker ELEXSYS E580 X-band spectrometer and a Magnettech L-band spectrometer. Immobilized EPR spectra in trehalose/sucrose were recorded at the University of Denver on a Bruker ELEXSYS E580 with X-band and Q-band capabilities. High-resolution mass spectrometry (HRMS) data were collected using a Thermo Fisher Scientific Q Exactive Mass Spectrometer with an electron spray ionization (ESI) source. High-performance liquid chromatography (HPLC) analyses were performed on a Waters Alliance e2695 separations module, equipped with a 2998 PDA detector. Separations were performed using a Waters XBridge BEH C18 4.6 mm × 50 mm, 2.5 μm column at 45 °C. All solvents were purchased from Fisher Scientific. All commercially available reagents were used as received without further purification. Tetrahydrofuran was purified on an Inert Pure Solv Solvent Purification system from Innovative Technologies Inc. Chloroform-^{13}C, 99 atom %, was purchased from MilliporeSigma. Glycerol (99.99%) was purchased from Acros Organics. All reactions were performed under argon in flame-dried glassware and in deoxygenated and anhydrous solvents. Solutions of **$^{13}C_1$−PTMTC** were protected from light.

Synthesis. *Tris(2,3,5,6-tetrachlorophenyl)methane-$^{13}C_1$ (**2**).* 1,2,4,5-Tetrachlorobenzene (8.06 g, 37.3 mmol, 9 equiv), aluminum(III) chloride (1.66 g, 12.4 mmol, 3 equiv), and chloroform ^{13}C 99% (500 mg, 4.1 mmol, 1 equiv) were added to a sealed pressure vessel and placed in a preheated bath (160 °C) for 2 h. The vessel was removed from the bath, then opened immediately, and 10 mL of both 5 M HCl and toluene were added to dissolve the mixture. The aqueous layer was extracted with 25 mL of toluene. Then the organic layer was washed with 10 mL of 1 M HCl (three times). The organic layer was dried over magnesium sulfate and filtered, and the solvent was evaporated under reduced pressure, then purified by flash chromatography on silica gel with hexanes to yield 833 mg of an off-white powder (33% yield based on $^{13}CHCl_3$ and 3% based on the 1,2,4,5-tetrachlorobenzene). ^{1}H NMR (400 MHz, $CDCl_3$) δ (ppm): 6.99 (d, J = 124 MHz, 1H, ^{13}C−H), 7.65 (s, 3H, Ar−H). ^{13}C NMR (100 MHz, $CDCl_3$) δ (ppm): 56.2 (C_1), 130.5 (C−Ar), 132.6 (C−Ar), 133.5 (C−Ar), 133.7 (C−Ar), 134.5 (C−Ar), 138.7 (d, J = 51 MHz, C−Ar). HRMS (ESI) m/z: $[M\text{-}H]^-$ calcd for $[C_{18}{}^{13}CH_3{}^{35}Cl_{12}]$ 651.6531, found 651.6538.

*Tris(4-methoxycarbonyl-2,3,5,6-tetrachlorophenyl)-methane-$^{13}C_1$ (**3**).* The triarylmethane **2** (685 mg, 1.04 mmol, 1 equiv) was dissolved in 68 mL of tetrahydrofuran and 1.56 mL of tetramethylethylenediamine (TMEDA) (1.22 g, 10.4 mmol, 10 equiv), then cooled to −78 °C. n-BuLi (6.51 mL, 10.4 mmol, 10 equiv, 1.6 M) was added to the chilled solution and mixed for 1 h. Methyl chloroformate (804 μL, 10.4 mmol, 10 equiv) was mixed in the solution at −78 °C for 10 min, then mixed for 1 h at room temperature. An additional 80 μL of methyl chloroformate was added and mixed for 1 h at room temperature. The tetrahydrofuran and TMEDA were evaporated under reduced pressure, and then the crude was dissolved in dichloromethane (15 mL). The organic layer was washed with 5 mL of water, 1 M HCl, and then water again. The organic layer was dried over magnesium sulfate and filtered, and the solvent was evaporated under reduced pressure. The solid was purified by flash chromatography on silica gel using hexanes/ethyl acetate to afford 407 mg (47%) of dark yellow solid. ^{1}H NMR (400 MHz, $CDCl_3$) δ (ppm): 4.01 (s, 9H, COO−CH_3), 7.01 (d, J = 120 MHz, 1H, ^{13}C−H). ^{13}C NMR (100 MHz, $CDCl_3$) δ (ppm): 53.1 (CH_3), 56.5 (C_1), 129.7 (C−Ar), 130.7 (C−Ar), 134.1 (C−Ar), 135.1 (C−Ar), 135.5 (C−Ar), 138.7 (d, J = 51 MHz, C−Ar), 163.8 (CO). HRMS (ESI) m/z $[M\text{-}H]^-$: calcd for $[C_{24}{}^{13}CH_9{}^{35}Cl_{12}O_6]$ 825.6695, found 825.6708.

*Tris(4-methoxycarbonyl-2,3,5,6-tetrachlorophenyl)methyl radical-$^{13}C_1$ (**4**).* To 10 mL of tetrahydrofuran, **3** (115 mg, 0.138 mmol) was added and shielded from light with aluminum foil. Benzyltetramethylammonium hydroxide solution in methanol (40% v/v, 121 μL, 0.276 mmol, 2 equiv) was added and mixed for 1 h. p-Chloranil (136 mg, 0.552 mmol, 4 equiv) was added to the solution and mixed for 3 h in dark conditions. The solvent was evaporated under reduced pressure, and the red solid was directly purified by flash chromatography on silica gel using hexanes/ethyl acetate to afford 111 mg (97%) of red solid. HRMS (ESI) m/z $[M]^-$: calcd for $[C_{24}{}^{13}CH_9{}^{35}Cl_{12}O_6]$ 825.6695, found 825.6706.

*Tris(4-carboxy-2,3,5,6-tetrachlorophenyl)methyl radical-$^{13}C_1$ sodium salt ([**$^{13}C_1$, 99%**]-**PTMTC**).* **4** (140 mg, 0.168 mmol) was added to a flask with 17.5 mL of neat, concentrated sulfuric acid, then heated at 90 °C for 4 h. The reaction was cooled to room temperature. Then the mixture was slowly poured over cracked ice. The aqueous layer was extracted with 5 mL of diethyl ether (five times), and then the organic layers were dried over magnesium sulfate and filtered, and the solvent was evaporated under reduced pressure. Compound [**$^{13}C_1$, 99%**]-**PTMTC** was purified by reverse-phase flash chromatography on C18 silica using 1% trifluoroacetic acid in water/acetonitrile. The red powder containing 70% of [**$^{13}C_1$, 99%**]-**PTMTC** and 30% of its reduced triarylmethane analogue **PTMTC-H** (as determined by HPLC/UV) was freeze-dried, added to water, and titrated to pH 6.0 with NaOH, then freeze-dried again to afford 115 mg (58%) of the sodium salt of [**$^{13}C_1$, 99%**]-**PTMTC** as a red powder. HRMS (ESI) m/z $[M]^-$: calcd for $[C_{21}{}^{13}CH_3{}^{35}Cl_{12}O_6]$ 783.6225, found 783.6186.

Sample Preparation and EPR Measurements in Aqueous Glycerol. Samples of [**$^{13}C_1$, 99%**]-**PTMTC** were prepared in 0, 12.5, 25, 35, 45, 67.5, 80, 85, 90% glycerol (%V/V) in water (Table S1). Concentrations are based on 70% [**$^{13}C_1$, 99%**]-**PTMTC**/30% [**$^{13}C_1$, 99%**]-**PTMTC-H** as determined by HPLC/UV. The final concentration of [**$^{13}C_1$, 99%**]-**PTMTC** was 400 μM based on the radical concentration. For the X-band

https://doi.org/10.1021/acs.jpcb.1c03778
J. Phys. Chem. B 2021, 125, 7380−7387

spectra: gas-permeable Teflon tubes (Zeus, Inc.) (I.D. 1.14 mm) with a 60 μm wall thickness were filled with 50 μL of sample and sealed with Kimble Cha-Seal. The temperature of the sample was maintained at 21.2 °C, and oxygen was removed from the sample by a steady flow of nitrogen for 20 min using a gas and temperature controller (Noxygen). Acquisition parameters were as follows: microwave power, 1 mW (except 0.1 mW for 0% glycerol); modulation amplitude, 2 G (except 0.5 G for 0% glycerol, 0.7 G for 12.5% glycerol, 1 G for 25% glycerol, and 1.5 G for 35% glycerol); modulation frequency, 100 kHz; sweep width, 150 G (full spectrum) and 60 G (high- and low-field peaks); sweep time, 81.92 s; conversion time, 40.00 ms; points, 2048; each spectrum was recorded in triplicate. The peak-to-peak line width of both the high- and low-field peaks at different viscosities are reported in Figure 5B, Table 2, and Table S2. For the L-band spectrum, 1 mL of the 400 μM [^{13}C$_1$, 99%]-**PTMTC** solution in water in a 3 mL Eppendorf was placed in the center of the resonator loop. The solution was bubbled with nitrogen for 30 min before acquisition. L-Band acquisition parameters were as follows; modulation amplitude, 0.8 G; modulation frequency, 100 kHz; sweep width, 150 G (full spectrum); sweep time, 60 s; conversion time; points, 2048; nonsaturating power; room temperature (~20 °C).

EPR Spectra of [^{13}C$_1$, 99%]-PTMTC Immobilized in Trehalose/Sucrose. 1.8 milligrams of solid trityl (70% [^{13}C$_1$, 99%]-**PTMTC**/30% [^{13}C$_1$, 99%]-**PTMTC-H**) was dissolved in 1.0 mL of 50 mM phosphate-buffered saline (PBS) at pH ≈ 7.2. A 2000:1 sugar/radical ratio was selected to give a high magnetic dilution. 0.34 grams of trehalose and 0.035 g of sucrose were mixed into the trityl solution in a 2.0 mL microfuge tube and then shaken and heated gently until a homogeneous solution was achieved. The solution was transferred by a micropipette to a watch glass, covered by an aluminum foil shell, and stored in a desk drawer to protect from light. After 3 d, a pink glass had formed that cracks easily. The glassy solid was placed in a 4 mm OD quartz tube for X-band and a 1.6 mm OD quartz capillary for Q-band. The X-band (9.6196 GHz) spectrum was acquired with a Bruker dielectric resonator, a modulation amplitude of 1.0 G, 100 kHz modulation frequency, and nonsaturating microwave power. The Q-band (33.8439 GHz) spectrum was acquired with a Bruker Q-band dielectric resonator, a modulation amplitude of 2.0 G, a modulation frequency of 100 kHz, and a nonsaturating microwave power.

Spectral Simulation. Spectra were simulated using Easyspin[23] ver. 5.2.28 and Matlab R2020b. The pepper function of Easyspin was used to fit the rigid spectra, while the chili function was used for the spectra recorded in water and water/glycerol mixtures. All spectra were simulated using g = [2.0015 2.0015 2.004] and A (MHz) = [26 25 199.5]. The hyperfine splitting in fluid solution was allowed to vary by 2 MHz to account for the experimental error and solvent dependence. The calculated hyperfine splittings for the ^{13}C satellites (see Table S3) were used as the initial guesses.

Computational Chemistry. The geometry of **PTMTC** was optimized at the UB3LYP/6-31G* level of theory using the ORCA 4.2.0 computational package.[24] The full Cartesian coordinates are given in the Supporting Information. The isotropic and anisotropic hyperfine splittings with ^{13}C were calculated using the "eprnmr" ORCA keyword for a single-point calculation using the IGLO-III basis sets for the optimized geometry.

Interaction with Bovine Serum Albumin. A 1 mM [^{13}C$_1$, 99%]-**PTMTC** in 1 mM aqueous bovine serum albumin (BSA) solution was prepared, and the spectrum was recorded at X-band under nitrogen flow using the following parameters. Microwave power, 1 mW; modulation amplitude, 0.9 G; modulation frequency, 100 kHz; sweep width, 150 G; sweep time, 81.92 s; conversion time, 40.00 ms; points, 2048.

RESULTS AND DISCUSSIONS

Elewa et al. reported a 50% enriched **^{13}C$_1$−PTMTC** that exhibits a doublet EPR spectrum in solution with an isotropic hyperfine coupling to the ^{13}C$_1$ of A_{iso} = 83.5 MHz (29.82 G).[22] This value is significantly higher than for the **^{13}C$_1$-dFT** analogue (A_{iso} = 65.38 MHz, 23.35G),[10,11] which indicates a higher spin density at the central carbon for **PTMTC** than for the Finland trityl derivative. This larger isotropic hyperfine splitting could lead to a higher spectral sensitivity to the probe tumbling if the anisotropy is proportionately larger for **^{13}C$_1$−PTMTC** than for **^{13}C$_1$-dFT**. However, the anisotropic values of the hyperfine interaction were not reported.[22] To get insight into the anisotropy of the ^{13}C$_1$ hyperfine interaction, we performed a density functional theory calculation at the B3LYP level using the IGLO-III basis sets, specially tailored for the calculation of EPR properties (Tables 1 and S3). The calculated isotropic hyperfine splitting of A_{iso} (C$_1$) = 77.6 MHz is in good agreement with the experimental value of 83.5 MHz.[22] The calculated A_x = A_y = 12.5 MHz and A_z = 208.0 MHz for the ^{13}C$_1$ supports a strong anisotropy of the hyperfine interaction and, therefore, high spectral sensitivity to the tumbling rate of the radical. The calculated hyperfine anisotropy $A_{\parallel} - A_{\perp}$ = 195.5 MHz (69 G) is higher than the A anisotropy for the **^{13}C$_1$-dFT** ($A_{\parallel} - A_{\perp}$ = 144 MHz, 52 G).[11]

Table 1. Experimental and Calculated A and g Values for ^{13}C$_1$−PTMTC

	experimental[a]	calculated UB3LYP/IGLO-III//UBL3LYP/6-31G*
A (MHz)	A_x = 26, A_y = 25, A_z = 199.5 A_{iso} = 83.5	A_x = 12.5, A_y = 12.5, A_z = 208.0 A_{iso} = 77.6
g[b]	g_x = g_y = 2.0015, g_z = 2.0040 g_{iso} = 2.0023	

[a]In trehalose/sucrose 9:1 at room temperature. [b]Although the differences between g values can be defined with uncertainties of ca. ±0.0002 in the simulations, absolute g values have uncertainties of ca. ±0.0004 due to the width of lines for radicals used in magnetic field calibrations.

To be used as a spin probe that is sensitive to molecular tumbling a **^{13}C$_1$−PTMTC** with higher than 50% ^{13}C enrichment is desirable for the maximum signal-to-noise ratio. Therefore, we synthesized 99% enriched **^{13}C$_1$−PTMTC** in a four-step sequence as depicted in Scheme 1. The synthetic strategy uses the procedures reported for **PTMTC** with minimal modifications and the use of a commercially available chloroform-^{13}C, 99 atom % ^{13}C to label the central carbon with 99% ^{13}C.[22,25,26] The sodium salt **^{13}C$_1$−PTMTC** was used throughout the study to ensure a high aqueous solubility. Since ion pairing is expected to be weak in aqueous solution and the pK_a for chlorinated benzoic acids is low, the dominant species in solution is the carboxylate anion.

The EPR spectrum of **^{13}C$_1$−PTMTC** (400 μM) was recorded at X-band (9.5 GHz) in deoxygenated water at room temperature (21.2 °C) (Figure 2A). The spectrum shows a large doublet arising from the hyperfine interaction with the ^{13}C$_1$ with an A_{iso} of 29.82G (83.5 MHz), in agreement with the

https://doi.org/10.1021/acs.jpcb.1c03778
J. Phys. Chem. B 2021, 125, 7380−7387

Scheme 1. Synthesis of [99%,$^{13}C_1$]-PTMTC

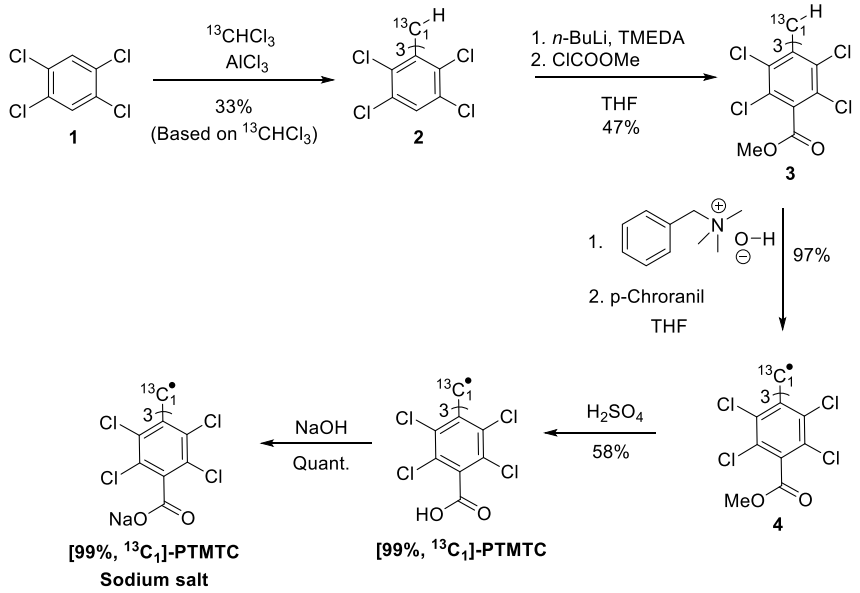

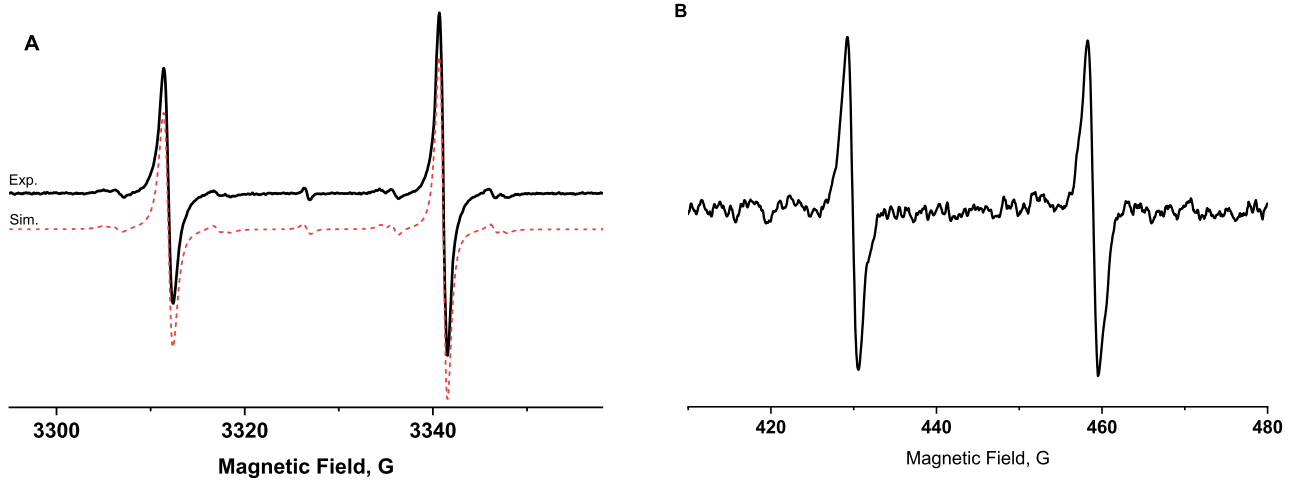

Figure 2. (A) X-Band spectrum (in black) of **$^{13}C_1$−PTMTC** 400 μM in deoxygenated water at room temperature. The spectrum was simulated (in red) using the chili function of EasySpin using the following parameters g = [2.0015 2.0015 2.0040], A_{C1} (MHz) = [26 25 199.5], log tcorr = −9.73, 90% contribution. The $C_{3,3'}$ and C_2 satellites were simulated using additional $A_{C3,3'}$ (MHz) = [26 26 37], 6% contribution and A_{C2} (MHz) = [33 33 41], 3% contribution, respectively. No hyperfine splittings were used to simulate the 1% contribution of **$^{12}C_1$−PTMTC**. (B) L-Band spectrum of the same solution.

previous report. The doublet is asymmetric with a broader low-field peak.[22] The peak-to-peak line widths for the low- and high-field peaks are 1.12 and 1.06 G. Additional lines corresponding to the ^{13}C satellites for $C_{3,3'}$ and C_2 1.1% natural abundance are also well-visible, while the ^{13}C satellites for the $C_{4,4'}$ and C_5 are not resolved. Also, the center of the spectrum features a single line corresponding to the 1% residual **$^{12}C_1$−PTMTC**. The low- and high-field peak line widths are significantly broader than for the **$^{12}C_1$−PTMTC**, which has a peak-to-peak line width of ∼0.4 G under similar conditions.[22] Those spectral features indicate an incomplete averaging of the A and g anisotropies by the molecular tumbling in water at room temperature. The same sample recorded at L-band (1.2 GHz) exhibits a symmetric doublet EPR spectrum in which both line widths are 1 G (Figure 2B). The lack of asymmetry for the L-band doublet confirms that an incomplete averaging of the g anisotropy of **$^{13}C_1$−PTMTC** is responsible for the asymmetry of the doublet at X-band.

Next, the **$^{13}C_1$−PTMTC** was immobilized in 9:1 trehalose/sucrose with a 2000:1 ratio of sugar to radical, and spectra were recorded at room temperature at X-band (Figure 3A) and Q-band (Figure 3B). The extrema of the large A_z are well-defined at X-band, which clearly defines the values of $g_z = 2.0040 \pm 0.0002$ and $A_z = 199.5 \pm 2$ MHz (Table 1). The relatively sharp perpendicular lines require the anisotropy to be small in the x,y-plane. On the basis of the X-band spectrum, it was concluded that $A_x = 26 \pm 2$ MHz, $A_y = 25 \pm 2$ MHz, and $g_x = g_y = 2.0015 \pm 0.0002$. The Q-band spectrum is an unusual case where there is an extensive overlap of the high-field A_z line with the perpendicular lines. The spectra at X-band and Q-band were simulated using the same A and g values, validating these parameters.

To study the influence of viscosity on the EPR spectra, we prepared solutions of **$^{13}C_1$−PTMTC** in water/glycerol mixtures and recorded the spectra at X-band. Figure 4 shows a progressive transition from a relatively narrow doublet at 0% glycerol to a

https://doi.org/10.1021/acs.jpcb.1c03778
J. Phys. Chem. B 2021, 125, 7380−7387

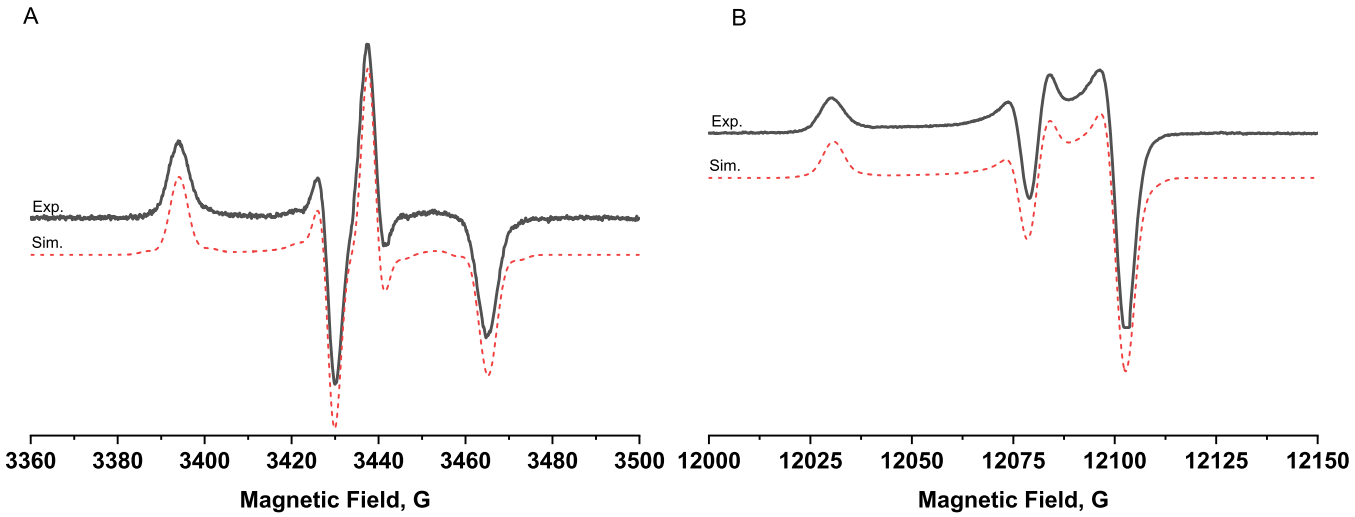

Figure 3. Spectra of $^{13}C_1$−**PTMTC** at room temperature immobilized in 9:1 trehalose/sucrose with a 2000:1 ratio of sugar to radical. (A) The X-band spectrum (in black) was simulated (in red) using the pepper function of EasySpin using the following parameters g = [2.0015 2.0015 2.0040], A C_1 (MHz) = [26 25 199.5], HStrain (MHz) = [11.5 11.5 13.5], 91% contribution. The $C_{3,3'}$ and C_2 satellites were simulated using additional A $C_{3,3'}$ (MHz) = [26 26 37], 6% contribution and A C_2 (MHz) = [33 33 41], 3% contribution, respectively. (B) The Q-Band spectrum (in black) was simulated (in red) using the pepper function of EasySpin using the same parameters as the X-band spectrum, except HStrain (MHz) = [16 16.5 17].

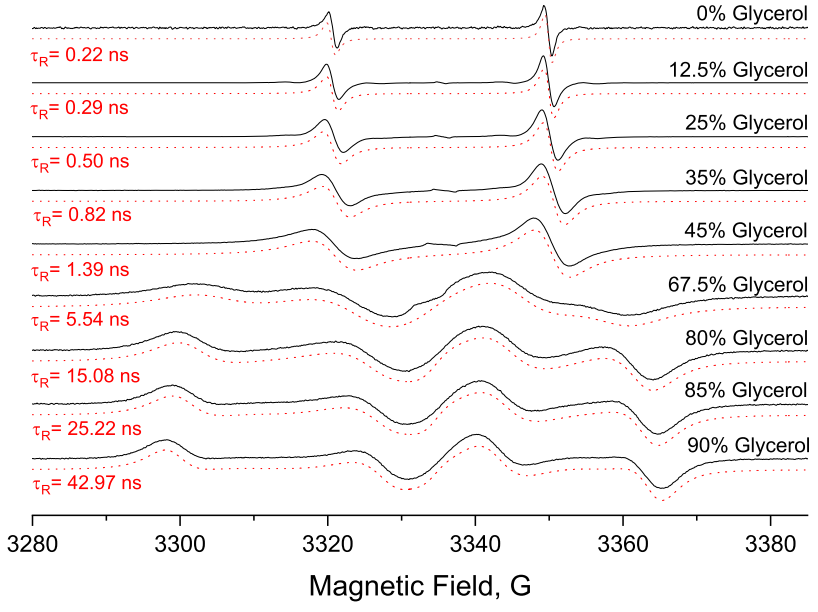

Figure 4. X-Band EPR spectra (in black) of $^{13}C_1$−**PTMTC** 400 μM in water/glycerol mixtures at 21.2 °C and simulated spectra (in red) with rotational correlation time (τ_R) determined using the chili function of EasySpin for $g_x = g_y = 2.0015$, $g_z = 2.0040$, $A_x = 26$, $A_y = 25$, $A_z = 199.5$ MHz.

rigid spectrum at 90% glycerol. Above 67.5% glycerol, 26.7 cP, the effect of viscosity on the X-band spectrum is relatively small, with only a slight increase of the apparent A_z. A spectral simulation using the chili function of EasySpin allows a determination for each solution of the rotational correlation time (τ_R) (Figure 4 and Table 2), which is defined as the time for the molecule to rotate by one radian.

Figure 5A shows the linear correlation between the τ_R determined by spectral simulations and the media viscosity. It is worth noting that the probe is sensitive to its microenvironment at the sub-micrometer scale.[4,27] The viscosity reported is, therefore, the microviscosity. Because of the lower spectral sensitivity at high viscosity (>30 cP), the accuracy of the τ_R determination is decreased for a viscosity value greater than 30 cP. The linear fit to τ_R versus viscosity leads to the equation τ_R(ns) = 0.21·viscosity(cP)+0.06 (for <30 cP). A spectral simulation of the EPR spectrum of $^{13}C_1$−**PTMTC** offers an accurate way to determine the probe τ_R and media microviscosity.

The Stokes−Einstein equation $\tau_R = \frac{V\eta}{kT}$ where V is the molecular volume, η is the viscosity, k is the Boltzmann's constant, and T is the temperature, theoretically correlates viscosity to τ_R. A molecular radius of 6.5 Å was estimated based on the optimized geometry of **PTMTC** at the UB3LYP/6-31G* level of theory (see the Supporting Information). With this molar volume, the Stokes−Einstein equation predicts a τ_R of 0.28 ns at 21 °C for **PTMTC** in water (0.98 cP). However, the

https://doi.org/10.1021/acs.jpcb.1c03778
J. Phys. Chem. B 2021, 125, 7380−7387

Table 2. Influence of Viscosity on τ_R Determined using EasySpin Simulations, on the Linewidths of the Doublet and on the Apparent A_z

glycerol[a] (%V/V)	viscosity (cP)	τ_R[b] (ns)	measured linewidth low-field peak[c] (G)	measured linewidth high-field peak[c] (G)	measured apparent A_z (G)
0	0.98	0.22 ± 0.04	1.12 ± 0.02	1.06 ± 0.03	
12.5	1.46	0.29 ± 0.03	1.66 ± 0.02	1.47 ± 0.02	
25	2.34	0.50 ± 0.03	2.57 ± 0.02	2.22 ± 0.02	
35	3.62	0.82 ± 0.01	3.85 ± 0.05	3.30 ± 0.04	
45	5.99	1.39 ± 0.01	6.05 ± 0.12	4.85 ± 0.12	
67.5	26.72	5.54 ± 0.01			58.67 ± 0.5
80	84.58	15.08 ± 0.19			64.38 ± 0.5
85	147.5	25.24 ± 0.98			66.06 ± 0.5
90	276	42.97 ± 1.71			67.31 ± 0.5

[a]%V/V Glycerol in deoxygenated water at 21.2 °C. [b]Mean of τ_R calculated from three individual spectra. [c]Mean of the peak-to-peak line widths measured from three spectra.

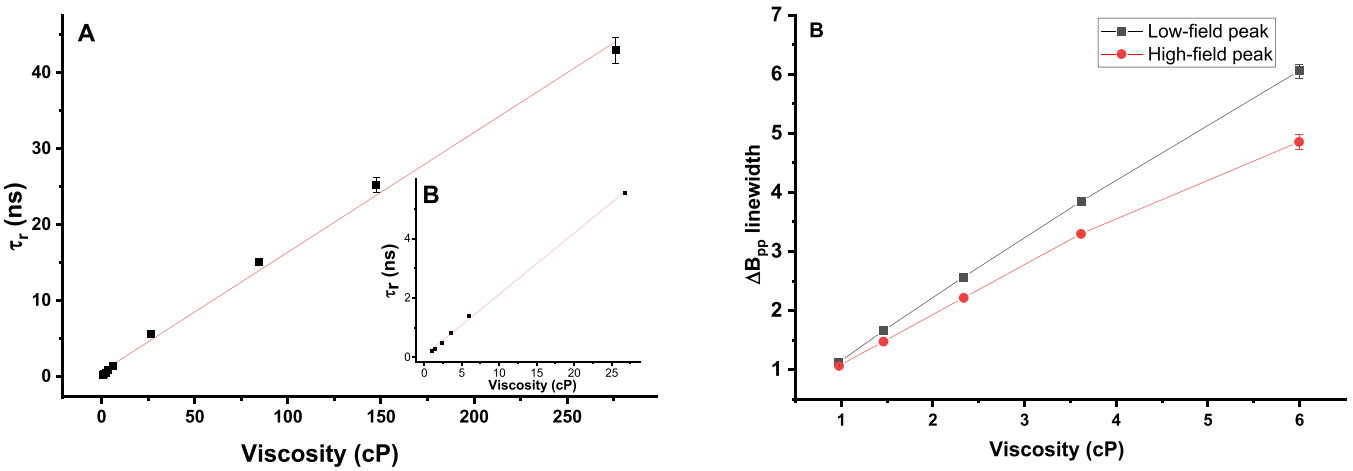

Figure 5. (A) τ_R (ns) from spectral simulations vs viscosity (cP). Linear fit leads to the equation $\tau R(ns) = 0.16 \cdot viscosity\ (cP) + 0.61$, $R^2 = 0.997$. (Inset B) τ_R (ns) vs viscosity (cP) for viscosity less than 30 cP, linear fit leads to the equation $\tau_R(ns) = 0.21 \cdot viscosity\ (cP) + 0.06$, $R^2 = 0.998$. (B) Measured ΔB_{pp} line widths for the low- and high-field peaks vs viscosity (cP). Linear fit below 4 cP leads to the equations $\Delta B_{pp}(G) = 1.03 \cdot viscosity\ (cP) + 0.14$, $R^2 = 0.999$ for high-field peak and $\Delta B_{pp}(G) = 0.84 \cdot viscosity\ (cP) + 0.24$, $R^2 = 1.000$ for the low-field peak.

predictions of the Stokes−Einstein model are better for solute molecules that are much larger than the solvent molecule.[28] For smaller molecules, the modified Stokes−Einstein equation $\tau_R = \frac{V\eta}{kT} C_{slip}$ with the addition of a slip coefficient (C_{slip}) was suggested to account for deviation from the model.[29,30] The experimental τ_R = 0.22 ns leads to a C_{slip} = 0.78, which is somewhat larger than the C_{slip} = 0.66 for **$^{13}C_1$-dFT**.[11]

Below 67.5% of glycerol (26.7 cP), the effect of viscosity on the X-band spectrum is a line broadening (Figure 4). This broadening is asymmetric between the two peaks because the anisotropy of the *g* tensor leads to a more substantial effect on the low-field peak (Table 2 and Figure 5B). The line widths can be calibrated versus τ_R or viscosity as a convenient way to extract those parameters without a spectral simulation.[10] For the low-field peak, the line width increases linearly with the viscosity for values up to 6 cP, while this relationship deviates from linearity at 4 cP for the high-field peak. The viscosity-induced line broadening of the low-field peak is 1.03G/cP, which is higher than for **$^{13}C_1$-dFT** (0.82 G/cP).[10] However, while the viscosity-induced line broadening is larger for **$^{13}C_1$−PTMTC** than for **$^{13}C_1$-dFT**, the relative change in line width is smaller because of the larger intrinsic line width of perchlorinated trityl radicals. Indeed, the broader lines for **$^{13}C_1$−PTMTC** than for **$^{13}C_1$-dFT** near the fast tumbling limit[10,11] are attributed to unresolved chlorine hyperfine couplings.[19] Molecular oxygen dissolved in the milieu also results in a broadening of the EPR lines of the probe through the Heisenberg spin exchange. However, the effect of oxygen is minimal by comparison to the viscosity. Indeed, the oxygen-induced line broadening for **PTMTC** is ∼0.5 mG/mmHg pO_2 in aqueous samples.[22] The maximum broadening due to the presence of dissolved oxygen is therefore ∼80 mG (pO_2 = 160 mmHg or 21%). Thus, oxygen could skew the EPR-determined microviscosity by only 0.1 cP, which is minimal. In addition, in vitro, the oxygen can easily be displaced inside the EPR cavity, while in vivo, the range of pO_2 is even smaller. Simulations have the advantage, relative to calculations based only on changes in line widths, that contributions to line widths such as oxygen broadening, concentration dependence, or overmodulation of the spectra that impact both hyperfine lines equally can be explicitly taken into account. Note that the equations that describe the dependence of continuous wave (CW) line widths on tumbling correlation times, anisotropic *g* values, and anisotropic *A* values that were derived for ^{15}N nitroxides can be used to analyze the line widths for the $^{13}C_1$ trityls.[31] The value of τ_R is calculated from the difference between the line widths of the high-field and low-field lines, which is proportional to the product of anisotropies in the *g* and *A* values. This method is less sensitive to τ_R than a simulation of the full line shape or calibrated analysis based on the line widths

https://doi.org/10.1021/acs.jpcb.1c03778
J. Phys. Chem. B 2021, 125, 7380−7387

for both hyperfine lines. Close to the rigid limit, for glycerol content above 67.5% (26.7 cP), the effect on the spectrum of an increased correlation time is an increase of the apparent A_z value. This value can also be used to estimate the τ_R and viscosity (Figures 4 and S1 and Table 2).

PTMTC is an amphiphilic molecule with a lipophilic tetrachlorotriarylmethyl core and three hydrophilic carboxylic acids. Therefore, **PTMTC** is expected to interact with biomacromolecules such as albumin through hydrophobic interactions.[32] On the one hand, the effect of a decrease of tumbling rate resulting from the interaction with a macromolecule on the EPR spectrum of **PTMTC** is expected to be small because of its single-line spectrum.[32] **$^{13}C_1$−PTMTC**, on the other hand, is highly sensitive to motion and could find an application in a study of molecular interactions. To demonstrate the effect of molecular interactions on the EPR spectrum of **$^{13}C_1$−PTMTC**, we prepared a solution of 1 mM **$^{13}C_1$−PTMTC** in 1 mM aqueous BSA, and the spectrum was recorded at X-band. Figure 6 clearly shows the presence of two spectral components—one sharp doublet (shown with asterisks) corresponding to unbound **$^{13}C_1$−PTMTC** in fast tumbling, and a more immobilized component (shown with black arrows), corresponding to **$^{13}C_1$−PTMTC** bound to the BSA. Note that a similar interaction with BSA was observed for the Finland trityl.[32] The correlation time of 38 ns extracted for the **$^{13}C_1$−PTMTC** bound to BSA is in good agreement with the 30 ns correlation time for BSA measured with a nitroxide probe.[33] In comparison, the τ_R predicted by the Stokes−Einstein models is 51 ns.[34]

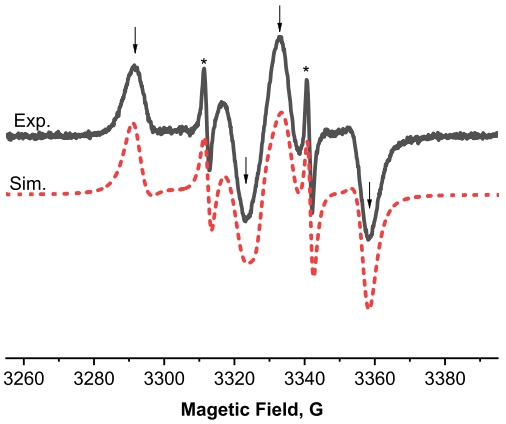

Figure 6. X-Band EPR spectrum (black) of **$^{13}C_1$−PTMTC** 1 mM in 1 mM BSA at room temperature. Simulated spectrum (red) based on two spectral components with τ_R = 0.30 ns and τ_R = 38 ns.

CONCLUSION

In conclusion, we have reported the synthesis of a 99% enriched **$^{13}C_1$−PTMTC** and its EPR characterization. The anisotropy of the A (A_x = 26, A_y = 25, A_z = 199.5 MHz) and the g (g_x = 2.0015, g_y = 2.0015, g_z = 2.0040) are responsible for a strong effect of the radical tumbling rate on the EPR spectrum. The rotational correlation time can be estimated by a spectral simulation and used to determine the local microviscosity. Alternatively, the line widths or the apparent A_z can be used as an empirical parameter to assess the probe rotational correlation time and microviscosity without a spectral simulation. We showed the EPR spectrum is strongly affected by the binding of **$^{13}C_1$−PTMTC** to BSA as a result of a lower tumbling rate of the radical when bound to the protein. Future developments and applications may include methanethiosulfonate (MTS) or maleimide derivatives of **$^{13}C_1$−PTMTC** for the labeling of protein through cysteine residues for structural biology studies. Compared to nitroxides, ^{13}C trityls exhibit narrower lines, resulting in a higher signal-to-noise ratio but are not yet commercially available. For future spin-labeling applications, one must consider that trityls are larger molecules than nitroxides and could potentially modify the structure of the biomacromolecules under investigation.

ASSOCIATED CONTENT

Supporting Information

The Supporting Information is available free of charge at https://pubs.acs.org/doi/10.1021/acs.jpcb.1c03778.

Sample preparation, NMR, HRMS and HPLC data, Cartesian coordinates for **PTMTC**, Experimental and calculated hyperfine splittings (PDF)

AUTHOR INFORMATION

Corresponding Author

Benoit Driesschaert − *Department of Pharmaceutical Sciences, West Virginia University, School of Pharmacy, Morgantown, West Virginia 26506, United States; In Vivo Multifunctional Magnetic Resonance Center, Robert C. Byrd Health Sciences Center, West Virginia University, Morgantown, West Virginia 26506, United States;* orcid.org/0000-0002-1402-413X; Email: benoit.driesschaert@hsc.wvu.edu

Authors

Justin L. Huffman − *Department of Pharmaceutical Sciences, West Virginia University, School of Pharmacy, Morgantown, West Virginia 26506, United States; In Vivo Multifunctional Magnetic Resonance Center, Robert C. Byrd Health Sciences Center, West Virginia University, Morgantown, West Virginia 26506, United States*

Martin Poncelet − *Department of Pharmaceutical Sciences, West Virginia University, School of Pharmacy, Morgantown, West Virginia 26506, United States; In Vivo Multifunctional Magnetic Resonance Center, Robert C. Byrd Health Sciences Center, West Virginia University, Morgantown, West Virginia 26506, United States*

Whylder Moore − *Department of Chemistry and Biochemistry, University of Denver, Denver, Colorado 80210, United States*

Sandra S. Eaton − *Department of Chemistry and Biochemistry, University of Denver, Denver, Colorado 80210, United States*

Gareth R. Eaton − *Department of Chemistry and Biochemistry, University of Denver, Denver, Colorado 80210, United States*

Complete contact information is available at: https://pubs.acs.org/10.1021/acs.jpcb.1c03778

Notes

The authors declare no competing financial interest.

ACKNOWLEDGMENTS

This work was partially supported by the National Institutes of Health (NIH), Grant Nos. (United States): NIBIB R00 EB023990 and NIBIB R21 EB028553 to B.D. and NCI R01 CA 177744 to G.R.E. and S.S.E. The content is solely the responsibility of the authors and does not necessarily represent the official views of the NIH. WVU HSC is acknowledged for start-up funds to B.D. The IMMR center and Prof. V. V.

Khramtsov are acknowledged for access to the EPR facility. EPR instruments were funded by the NIH, Grant No. NIGMS U54 GM104942.

REFERENCES

(1) Serda, M.; Wu, Y.-K.; Barth, E. D.; Halpern, H. J.; Rawal, V. H. EPR Imaging Spin Probe Trityl Radical OX063: A Method for Its Isolation from Animal Effluent, Redox Chemistry of Its Quinone Methide Oxidation Product, and in Vivo Application in a Mouse. *Chem. Res. Toxicol.* **2016**, *29* (12), 2153−2156.
(2) Marchand, V.; Levêque, P.; Driesschaert, B.; Marchand-Brynaert, J.; Gallez, B. In vivo EPR extracellular pH-metry in tumors using a triphosphonated trityl radical. *Magn. Reson. Med.* **2017**, *77* (6), 2438−2443.
(3) Khramtsov, V. V.; Grigor'ev, I. A.; Foster, M. A.; Lurie, D. J. In vitro and in vivo measurement of pH and thiols by EPR-based techniques. *Antioxid. Redox Signaling* **2004**, *6* (3), 667−76.
(4) Clark, A.; Sedhom, J.; Elajaili, H.; Eaton, G. R.; Eaton, S. S. Dependence of electron paramagnetic resonance spectral lineshapes on molecular tumbling: Nitroxide radical in water:glycerol mixtures. *Concepts Magn. Reson., Part A* **2016**, *45A* (5), No. e21423.
(5) Marsh, D. Spin-Label EPR for Determining Polarity and Proticity in Biomolecular Assemblies: Transmembrane Profiles. *Appl. Magn. Reson.* **2010**, *37* (1), 435−454.
(6) Ilangovan, G.; Li, H.; Zweier, J. L.; Kuppusamy, P. In vivo measurement of tumor redox environment using EPR spectroscopy. *Mol. Cell. Biochem.* **2002**, *234* (1), 393−398.
(7) Poncelet, M.; Driesschaert, B.; Bobko, A. A.; Khramtsov, V. V. Triarylmethyl-based biradical as a superoxide probe. *Free Radical Res.* **2018**, *52* (3), 373−379.
(8) Kutala, V. K.; Parinandi, N. L.; Zweier, J. L.; Kuppusamy, P. Reaction of superoxide with trityl radical: implications for the determination of superoxide by spectrophotometry. *Arch. Biochem. Biophys.* **2004**, *424* (1), 81−88.
(9) Halpern, H. J.; Chandramouli, G. V. R.; Barth, E. D.; Yu, C.; Peric, M.; Grdina, D. J.; Teicher, B. A. Diminished Aqueous Microviscosity of Tumors in Murine Models Measured with in Vivo Radiofrequency Electron Paramagnetic Resonance. *Cancer Res.* **1999**, *59* (22), 5836−5841.
(10) Poncelet, M.; Driesschaert, B. A 13C-Labeled Triarylmethyl Radical as an EPR Spin Probe Highly Sensitive to Molecular Tumbling. *Angew. Chem., Int. Ed.* **2020**, *59* (38), 16451−16454.
(11) Moore, W.; McPeak, J. E.; Poncelet, M.; Driesschaert, B.; Eaton, S. S.; Eaton, G. R. 13C isotope enrichment of the central trityl carbon decreases fluid solution electron spin relaxation times. *J. Magn. Reson.* **2020**, *318*, 106797.
(12) Velayutham, M.; Poncelet, M.; Eubank, T. D.; Driesschaert, B.; Khramtsov, V. V. Biological Applications of Electron Paramagnetic Resonance Viscometry Using a 13C-Labeled Trityl Spin Probe. *Molecules* **2021**, *26* (9), 2781.
(13) Boś-Liedke, A.; Walawender, M.; Woźniak, A.; Flak, D.; Gapiński, J.; Jurga, S.; Kucińska, M.; Plewiński, A.; Murias, M.; Elewa, M.; Lampp, L.; Imming, P.; Tadyszak, K. EPR Oximetry Sensor—Developing a TAM Derivative for In Vivo Studies. *Cell Biochem. Biophys.* **2018**, *76* (1), 19−28.
(14) Bratasz, A.; Kulkarni, A. C.; Kuppusamy, P. A Highly Sensitive Biocompatible Spin Probe for Imaging of Oxygen Concentration in Tissues. *Biophys. J.* **2007**, *92* (8), 2918−2925.
(15) Dang, V.; Wang, J.; Feng, S.; Buron, C.; Villamena, F. A.; Wang, P. G.; Kuppusamy, P. Synthesis and characterization of a perchlorotriphenylmethyl (trityl) triester radical: A potential sensor for superoxide and oxygen in biological systems. *Bioorg. Med. Chem. Lett.* **2007**, *17* (14), 4062−4065.
(16) Kutala, V. K.; Villamena, F. A.; Ilangovan, G.; Maspoch, D.; Roques, N.; Veciana, J.; Rovira, C.; Kuppusamy, P. Reactivity of Superoxide Anion Radical with a Perchlorotriphenylmethyl (Trityl) Radical. *J. Phys. Chem. B* **2008**, *112* (1), 158−167.
(17) Mesa, J. A.; Chávez, S.; Fajarí, L.; Torres, J. L.; Juliá, L. A tri(potassium sulfonate) derivative of perchlorotriphenylmethyl radical (PTM) as a stable water soluble radical-scavenger of the hydroxyl radical more powerful than 5,5-dimethyl-1-pyrroline-N-oxide. *RSC Adv.* **2013**, *3* (25), 9949−9956.
(18) Banerjee, D.; Paniagua, J. C.; Mugnaini, V.; Veciana, J.; Feintuch, A.; Pons, M.; Goldfarb, D. Correlation of the EPR properties of perchlorotriphenylmethyl radicals and their efficiency as DNP polarizers. *Phys. Chem. Chem. Phys.* **2011**, *13* (41), 18626−18637.
(19) Paniagua, J. C.; Mugnaini, V.; Gabellieri, C.; Feliz, M.; Roques, N.; Veciana, J.; Pons, M. Polychlorinated trityl radicals for dynamic nuclear polarization: the role of chlorine nuclei. *Phys. Chem. Chem. Phys.* **2010**, *12* (22), 5824−5829.
(20) Kimura, S.; Matsuoka, R.; Kimura, S.; Nishihara, H.; Kusamoto, T. Radical-Based Coordination Polymers as a Platform for Magneto-luminescence. *J. Am. Chem. Soc.* **2021**, *143* (15), 5610−5615.
(21) Kimura, S.; Uejima, M.; Ota, W.; Sato, T.; Kusaka, S.; Matsuda, R.; Nishihara, H.; Kusamoto, T. An Open-shell, Luminescent, Two-Dimensional Coordination Polymer with a Honeycomb Lattice and Triangular Organic Radical. *J. Am. Chem. Soc.* **2021**, *143* (11), 4329−4338.
(22) Elewa, M.; Maltar-Strmečki, N.; Said, M. M.; El Shihawy, H. A.; El-Sadek, M.; Frank, J.; Drescher, S.; Drescher, M.; Mäder, K.; Hinderberger, D.; Imming, P. Synthesis and EPR-spectroscopic characterization of the perchlorotriarylmethyl tricarboxylic acid radical (PTMTC) and its 13C labelled analogue (13C-PTMTC). *Phys. Chem. Chem. Phys.* **2017**, *19* (9), 6688−6697.
(23) Stoll, S.; Schweiger, A. EasySpin, a comprehensive software package for spectral simulation and analysis in EPR. *J. Magn. Reson.* **2006**, *178* (1), 42−55.
(24) Neese, F. Software update: the ORCA program system, version 4.0. *Wiley Interdiscip. Rev.: Comput. Mol. Sci.* **2018**, *8* (1), No. e1327.
(25) Frank, J.; Elewa, M.; M Said, M.; El Shihawy, H. A.; El-Sadek, M.; Müller, D.; Meister, A.; Hause, G.; Drescher, S.; Metz, H.; Imming, P.; Mäder, K. Synthesis, Characterization, and Nanoencapsulation of Tetrathiatriarylmethyl and Tetrachlorotriarylmethyl (Trityl) Radical Derivatives—A Study To Advance Their Applicability as in Vivo EPR Oxygen Sensors. *J. Org. Chem.* **2015**, *80* (13), 6754−6766.
(26) Ballester, M.; Riera, J.; Castañer, J.; Rovira, C.; Armet, O. An Easy, High-yield Synthesis of Highly Chlorinated Mono-, Di- and Triarylmethanes. *Synthesis* **1986**, *1986* (01), 64−66.
(27) Morse, P. D.; Lusczakoski, D. M.; Simpson, D. A. Internal microviscosity of red blood cells and hemoglobin-free resealed ghosts: a spin-label study. *Biochemistry* **1979**, *18* (22), 5021−5029.
(28) Percival, P. W.; Hyde, J. S. Saturation-recovery measurements of the spin-lattice relaxation times of some nitroxides in solution. *J. Magn. Reson.* **1976**, *23* (2), 249−257.
(29) Kivelson, D.; Madden, P. A. Light Scattering Studies of Molecular Liquids. *Annu. Rev. Phys. Chem.* **1980**, *31* (1), 523−558.
(30) McClung, R. E. D.; Kivelson, D. ESR Linewidths in Solution. V. Studies of Spin−Rotational Effects Not Described by Rotational Diffusion Theory. *J. Chem. Phys.* **1968**, *49* (8), 3380−3391.
(31) Gaffney, B. J.; Elbrecht, C. H.; Scibilia, J. P. A. Enhanced sensitivity to slow motions using 15N-nitroxide spin labels. *J. Magn. Reson.* **1981**, *44* (3), 436−446.
(32) Song, Y.; Liu, Y.; Liu, W.; Villamena, F. A.; Zweier, J. L. Characterization of the binding of the Finland trityl radical with bovine serum albumin. *RSC Adv.* **2014**, *4* (88), 47649−47656.
(33) Cobb, C. E.; Hustedt, E. J.; Beechem, J. M.; Beth, A. H. Protein rotational dynamics investigated with a dual EPR/optical molecular probe. Spin-labeled eosin. *Biophys. J.* **1993**, *64* (3), 605−613.
(34) Gelamo, E. L.; Itri, R.; Alonso, A.; da Silva, J. V.; Tabak, M. Small-angle X-ray scattering and electron paramagnetic resonance study of the interaction of bovine serum albumin with ionic surfactants. *J. Colloid Interface Sci.* **2004**, *277* (2), 471−482.

https://doi.org/10.1021/acs.jpcb.1c03778
J. Phys. Chem. B 2021, 125, 7380−7387